




Computational modeling of targeted temperature management in post-cardiac arrest patients

Maja Duh¹ · Kristijan Skok^{2,3} · Matjaž Perc^{1,4,5,6} · Andrej Markota^{2,7} · Marko Gosak^{1,2} 

Received: 27 February 2022 / Accepted: 23 May 2022 / Published online: 28 June 2022

© The Author(s), under exclusive licence to Springer-Verlag GmbH Germany, part of Springer Nature 2022

Abstract

Our core body temperature is held around 37 °C by an effective internal thermoregulatory system. However, various clinical scenarios have a more favorable outcome under external temperature regulation. Therapeutic hypothermia, for example, was found beneficial for the outcome of resuscitated cardiac arrest patients due to its protection against cerebral ischemia. Nonetheless, practice shows that outcomes of targeted temperature management vary considerably in dependence on individual tissue damage levels and differences in therapeutic strategies and protocols. Here, we address these differences in detail by means of computational modeling. We develop a multi-segment and multi-node thermoregulatory model that takes into account details related to specific post-cardiac arrest-related conditions, such as thermal imbalances due to sedation and anesthesia, increased metabolic rates induced by inflammatory processes, and various external cooling techniques. In our simulations, we track the evolution of the body temperature in patients subjected to post-resuscitation care, with particular emphasis on temperature regulation via an esophageal heat transfer device, on the examination of the alternative gastric cooling with ice slurry, and on how anesthesia and the level of inflammatory response influence thermal behavior. Our research provides a better understanding of the heat transfer processes and therapies used in post-cardiac arrest patients.

Keywords Thermoregulation · Human thermal model · Targeted temperature management · Cardiac arrest · Intensive care · Bio-heat transfer · Hypothermia

1 Introduction

Humans maintain a constant temperature, which is normally referred to as the core body temperature and lies within 36 – 37.5 °C, whereas the extremities or peripheral shell temperatures are usually around 4 °C lower than core body temperature (Morrison and Nakamura 2019; Tansey and Johnson 2015). The human body is striving to maintain homeostasis of all bodily functions. This includes thermal balance, which depends on several physical and physiological events (Wang et al. 2016). The interconnectedness of these events implies that the body is thermally balanced when, expressed in mathematical terms, the heat storage is zero. It is evident that for a sustained and regulated core temperature, thermoregulation has to be kept in a dynamic balance between heat production/gain and heat loss (Tansey and Johnson 2015). It should be noted that there are several pathological states that can lead to thermal imbalances of the human body. These can be as simple as a fever due to a mild infection or extremely high fever (hyperpyrexia; > 41.5 °C) due to sepsis or even as part of the post-cardiac

✉ Marko Gosak
marko.gosak@um.si

¹ Faculty of Natural Sciences and Mathematics, University of Maribor, Koroška cesta 160, 2000 Maribor, Slovenia

² Faculty of Medicine, University of Maribor, Taborska ulica 8, 2000 Maribor, Slovenia

³ Department of Pathology, General Hospital Graz II, Location West, Göstinger Straße 22, 8020 Graz, Austria

⁴ Department of Medical Research, China Medical University Hospital, China Medical University, Taichung 404332, Taiwan

⁵ Alma Mater Europaea, Slovenska ulica 17, 2000 Maribor, Slovenia

⁶ Complexity Science Hub Vienna, Josefstädterstraße 39, 1080 Vienna, Austria

⁷ Medical Intensive Care Unit, University Medical Centre Maribor, Ljubljanska 5, 2000 Maribor, Slovenia

arrest syndrome, which is tackled with targeted temperature management (TTM) strategies (Lascarrou et al. 2019). The latter presents one of the most important research areas in critical care medicine and therapeutic thermoregulation.

Temperature modulation in comatose survivors after cardiac arrest consists of induction of mild hypothermia or maintenance of normothermia. In these patients' fever is associated with increased mortality (Donnino et al. 2015; Nolan et al. 2015). Several opposing factors contribute to temperature changes after cardiac arrest. Systemic inflammatory response syndrome that develops after cardiac arrest leads to increased body temperature. There are several pathophysiological mechanisms that occur after resuscitation from cardiac arrest, which are united under the term called post-cardiac arrest syndrome. This syndrome comprises four parts: a) the primary pathological state that led to cardiac arrest; b) cerebral hypoperfusion with ischemia–reperfusion injury; c) myocardial dysfunction after a return of spontaneous circulation and d) systemic ischemia/reperfusion response (Skok et al. 2020; Leong et al. 2017; Markota et al. 2022; Alves and Mady 2020). In order to achieve a decrease in temperature (or to maintain normothermia), several interventions aimed at cooling need to be utilized: physical cooling (internal and/or external) and pharmacological interventions (e.g., acetaminophen), but effects of other medications that are required in this patient population also need to be considered (e.g., intravenous sedation and opiate analgesia). In addition to changes in body temperature, all interventions above have side effects with important clinical implications: for example, hypovolemia and hypokalemia are associated with increased urine output, increased susceptibility to infections, or complications associated with devices used to manage temperature. Despite strict protocols (hypothermia range from 32 °C to 34 °C), there is still a large variability in patient behavior even if they are subjected to very similar protocols. This is not only due to inter-individual variability but also due to different levels of organ damage, leading to more intense inflammatory response, etc. (Donnino et al. 2015; Nolan et al. 2015).

The desired temperature can be regulated by different means and devices. Cooling via surface methods, such as ice packs, blankets and air-cooling is relatively simple, noninvasive and cheap, but not very effective (Nolan et al. 2015). In contrast, internal methods such as intravascular cooling directly affect the core body temperature and are therefore more efficient, but might lead to serious side effects (Kim et al. 2018). Noteworthy, in recent years several minimally invasive methods have been developed, such as esophageal or nasal cavity cooling devices (Goury et al. 2017; Naiman et al. 2016; Hegazy et al. 2017; Badjatia et al. 2020). The esophageal heat transfer device (EHTD) has been in use since 2015 and has proven out to be effective for TTM in cardiac arrest patients (Hegazy

et al. 2015; Markota et al. 2016). Its main advantages are anatomical location in vicinity of great vessels and heart, enabling contact with blood in central circulation, and minimally invasive insertion—insertion of a gastric tube is a common procedure. Moreover, adequate sedation and use of neuromuscular blocking agents facilitate the insertion of the EHTD (Leong et al. 2017; Nguyen et al. 2018). While the efficacy and safety of the EHTD has been previously proven, there is still a lack of information on the optimal usage setting and protocol (Goury et al. 2017; Khan et al. 2018; Naiman et al. 2017).

To address the complexity of the human thermal system, computational thermoregulatory models have been developed, as a means to better understand and predict the thermal responses in different environmental conditions and circumstances (Fiala et al. 2010; Katič et al. 2016; Fu et al. 2016; Enescu 2019). In these models, the human body is typically represented by two interacting systems of thermoregulation: (1) the controlling active system, which represents thermoregulatory responses of vasoconstriction, vasodilation, shivering, sweating, and metabolic heat production, and (2) the controlled passive systems, which resembles thermal interactions between the body, the environment and the heat transfer within the body (Fu et al. 2016). Mathematical modeling of the human thermal system has a long tradition (Pennes 1948; Gagge et al. 1971; Stolwijk 1970). During the past forty years, the initial relatively simple models have evolved to more sophisticated, multi-segmental and multi-node models, which are based on the theories of physiology, thermodynamics and transport processes and aim to predict the thermal behavior of either the entire human body or a part of it. Individual segments are typically cylindrical elements that mimic different parts of the body and are interconnected through blood flow, whereas each segment is divided into different nodes between which heat is transferred (Fu et al. 2016; Hensley et al. 2013). Various strategies have been used for the compartmentalization of segments. In more elementary schemes, each body element is composed of the core, skin and blood nodes, whereas in more detailed models each segment is built of annular concentric tissue layers with different thermal properties (Fiala et al. 2010). Recent endeavors focus on very specific aspects of thermophysiological modeling, such as detailed descriptions of the cardiovascular or respiratory systems (Shrivastava 2018), interindividual variability (Zhang et al. 2001), or the incorporation of specific environmental conditions (Jiang et al. 2010; Weng et al. 2014). With the skin and core temperatures as the main output variables these models offer numerous applications and have till now been mostly used the context of thermal comfort research and sensation, with emphasis on automotive research, clothing and building simulation (Enescu 2019; Fiala et al. 2010; Koelblen et al. 2017).

Computational thermoregulation models are increasingly gaining attention also in the framework of biomedical applications (Shafirstein and Feng 2013; Shrivastava 2018; Skok et al. 2020). A substantial part of the endeavors is devoted to the description of local heat transfer in tissues with the aim to predict the relationship between dosages and impact of deposited thermal energy. Examples include interstitial laser thermal therapies (Fuentes et al. 2009), microwave thermal ablations (Faridi and Prakash 2018), ultrasound thermotherapy (Prakash et al. 2013), and nanoparticle-mediated hyperthermal cancer therapy (Kaddi et al. 2013; Raouf et al. 2020; Orthaber et al. 2017), including the magnetic fluid hyperthermia (Suriyanto and Kumar 2017), to name only a few. Moreover, increasing effort is given to the utilization whole-body thermal models in various contexts of thermal medicine. Simulations have been performed to evaluate different surface-based cooling and rewarming techniques, such as cooling mattress (Bräuer et al. 2004; Silva et al. 2018), air-cooling (Romadhon et al. 2017; Wakamatsu and Utsuki 2009), postoperative rewarming with blankets (Vallez et al. 2016), and specialized temperature management systems (Vanlandingham et al. 2015; Wang et al. 2021). Similarly, others have utilized mathematical models to investigate the effectiveness of cooling with peripheral infusions of coolants (Rosengart et al. 2009; Neimark et al. 2008) and to predict the temperature variations induced by intravascular cooling (van Willigen et al. 2019; Xue and Liu 2011) or via an esophageal route (Vaicys et al. 2012; Williams et al. 2016). Intensive care unit (ICU) patients are usually sedated, and consequently, their thermoregulatory system is impaired. Anesthesia does not only decrease basal metabolic levels but also shifts the thresholds for sweating, vasoconstriction, and shivering, which results in dose- and time-dependent hypothermia (Sessler 1997). Till today, very few studies have explored theoretically modifications of thermoregulatory principles during anesthesia and surgical procedures. In 2008 Tindall et al. (2008) proposed a rather phenomenological model to examine heat transfer processes between the core organs and peripheral body parts in patients undergoing cardiac surgery, with emphasis on how proper post rewarming protocols can prevent the afterdrop of the core temperatures. A more detailed multi-segment and multi-node model was developed by Severens et al. (2007), with the aim to predict the patient temperature during cardiac surgery. The main advantage of their computational work was the incorporation of the pharmacological effect of the anesthetic on various physiological functions, such as metabolism and blood flow rates, which crucially affect the thermal balance and must be considered to achieve agreement with measured data.

A typical successfully resuscitated cardiac arrest patient is subjected to a series of procedures to prevent hyperthermia and, later in the process, to induce mild hypothermia.

At first, patients are usually treated with cold fluid infusion and cooling blankets even before hospital administration. Following a series of diagnostic procedures, patients are admitted to the ICU where TTM continues. For this purpose, different methods and devices to induce hypothermia are available and the choice often relies on local experience and logistics. In recent years, also novel semi-invasive methods such as the EHTD are gaining on popularity and their optimal implementation has yet to be determined. Nevertheless, to the best of our knowledge, no detailed biothermal model has been proposed which would incorporate the cascade of processes and modified thermoregulatory responses encompassed in post-cardiac arrest management care. In the present study, we aim to address these issues by designing such a computational model in order to examine the thermal responses of patients in these specific clinical circumstances. Particular emphasis is given to TTM via the EHTD and to the possibility to induce mild hypothermia with ice slurry gastric cooling.

2 Mathematical model

To model the thermal and regulatory responses of the human body under various personal and environmental conditions, we develop a multi-segment and multi-node model based on the framework proposed by Salloum et al. (2007), which we complemented with several completions in order to simulate specific clinical scenarios. The scheme of the model is presented in Fig. 1, whereas a detailed description of particular components is given in continuation.

The model divides the body into the fifteen cylindrical body segments: head, trunk, pelvis, upper arms, forearms, hands, thighs, calves and feet. Each of these segments consists of four nodes, representing core, skin, artery blood, and vein blood. The segments are connected through the blood flow in the arteries and veins which leads to a distribution of heat within the body. Following the Avolio multi-branched model of the human arterial system (Avolio 1980), the human circulatory system is represented by 128 arteries sorted by body segments. The vessels are represented by uniform thin-walled elastic tubes with realistic dimensions and anatomic positions in the body. The details of length and diameter of each vessel can be found in Avolio's work (Avolio 1980).

2.1 Energy balance equations

To describe the heat transfer between the body and the environment, as well as inside the body itself, energy balance equations are derived for each of the four nodes separately (Salloum et al. 2007). After some modifications of the

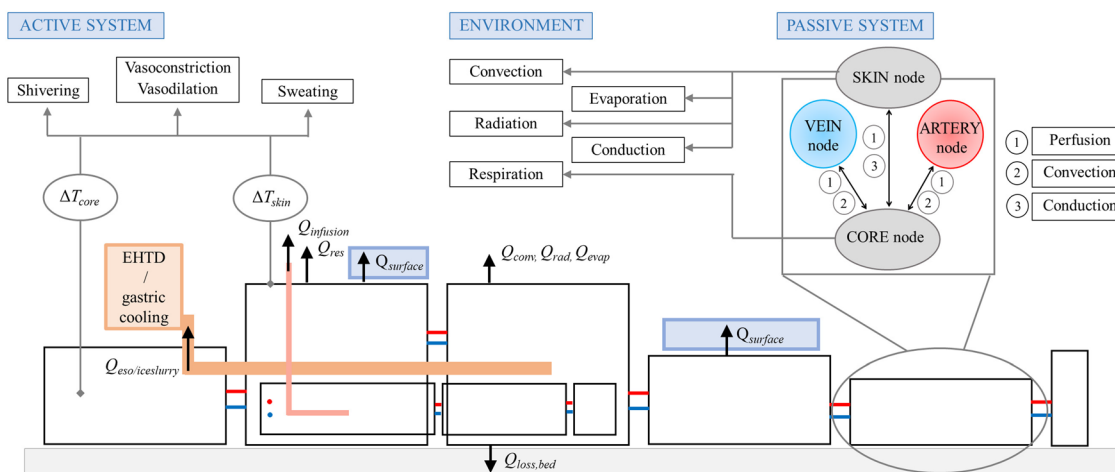


Fig. 1 A schematic representation of a thermophysiological computational model for predicting human thermal and regulatory responses in the ICU. Each of the 15 cylindrical segments represents different body parts and is divided into four nodes: core, skin, arterial, and venous blood. Within individual segments, heat is transferred between nodes by perfusion (1), convection (2) and conduction (3), i.e., passive system, and individual segments are connected through blood flow in the arteries and veins to account for the transportation of heat inside the body. Vasoconstriction, vasodilation and sweating along with metabolic heat production within the core keep the body in thermal balance with respect to the heat exchange with the envi-

ronment. In the ICU, the heat balance of the patient is additionally influenced by different methods of TTM (surface cooling, infusions of cold saline, cooling devices), leading to regulated hypothermia. Abbreviations: $Q_{surface}$, surface body cooling; $Q_{loss,bed}$, conductive heat loss through the bed; Q_{conv} , Q_{rad} , and Q_{evap} , heat exchange with the environment by convection, radiation, and evaporation; Q_{res} , respiratory heat loss; $Q_{infusion}$, heat exchange due to intravenous saline infusion; $Q_{eso/iceslurry}$, heat exchange between the body core and EHTD or gastric ice slurry; EHTD, esophageal heat transfer device; ΔT_{core} , change in body core temperature; ΔT_{skin} , change in skin temperature (see main text for further details)

original model, the energy balance equations of the layers in a specific body segment can be expressed as:

$$C_{cr} \frac{dT_{cr}}{dt} = M_{cr} + Q_{res} + Q_{cr-sk} + Q_{cr-art} + Q_{cr-vein} + Q_{cr-art,per} + Q_{sk,per} \quad (1)$$

$$C_{sk} \frac{dT_{sk}}{dt} = M_{sk} + Q_{cr-sk} + Q_{sk,per} + Q_{conv} + Q_{rad} + Q_{evap} \quad (2)$$

$$C_{bl,a} \frac{dT_{bl,a}}{dt} = Q_{cr-art} + Q_{adj,a} \quad (3)$$

$$C_{bl,v} \frac{dT_{bl,v}}{dt} = Q_{cr-vein} + Q_{adj,v} + Q_{cr-vein,per} \quad (4)$$

where C_{cr} , C_{sk} , $C_{bl,a}$ and $C_{bl,v}$ are the heat capacitances of the core, skin, artery and vein node, obtained from Salloum et al. (2007), T_{cr} , T_{sk} , $T_{bl,a}$ and $T_{bl,v}$ are the temperatures of the four nodes, and t denotes the time. M_{cr} and M_{sk} are the metabolic rates in the core and skin node composed of the basal metabolic rate (M_0) and an additional heat gain (ΔM) as described further below. $Q_{res} = 0.0014M(34 - T_{amb}) + 0.0173M(5.87 - P_{amb})$ is the respiratory heat loss (ASHRAE 2001), which is supposed

to occur only in the core layer of the chest segment, where T_{amb} is the ambient temperature in °C and P_{amb} is the ambient vapor pressure in kPa. $Q_{cr-sk} = K(T_{cr} - T_{sk})$ is the heat exchange between the core and skin by conduction, where K is the skin conductance given for each body segment taken from Salloum et al. (2007).

$Q_{cr-art} = [\sum_{arteries} h_{bl} A_{artery}] (T_{cr} - T_{bl,a})$ and $Q_{cr-vein} = [\sum_{veins} h_{bl} A_{vein}] (T_{cr} - T_{bl,v})$ are the heat exchanges by convection between the core and artery node in the first term and between the core and vein node in the second term. h_{bl} is the convective heat transfer coefficient of blood, taken as 984 W/(m²K) (Holopainen 2012), and A_{artery}/A_{vein} is the inner surface area of an artery/vein vessel, respectively. The details of length and diameter of each blood vessel can be found in Avolio's work (Avolio 1980). Furthermore, the vein diameter is assumed equal to twice its corresponding artery diameter. The summation of the product of the convection heat transfer coefficient and surface area is performed over all the blood vessel branches of the segment under consideration.

$Q_{cr-art,per} = \dot{m}_{per,tot} c_{bl} (T_{bl,a} - T_{cr})$ and $Q_{cr-vein,per} = \dot{m}_{per,tot} c_{bl} (T_{cr} - T_{bl,v})$ are the heat flows associated with perfusion blood flow in the core, where $\dot{m}_{per,tot}$ is the total perfusion rate of blood entering the core node and c_{bl} is the specific heat of blood, taken as 4000 J/(kgK) (Salloum et al. 2007). The blood is then flowing from the core into the skin layer, where heat exchange between the core and

the skin associated with the skin perfusion blood flow rate (\dot{m}_{sk}) is given by $Q_{sk,per} = \dot{m}_{sk} c_{bl}(T_{sk} - T_{cr})$. The blood mass flow rates and their alterations in specific circumstances are described further below.

The skin node exchange heat with the environment by convection (Q_{conv}), radiation (Q_{rad}), and evaporation (Q_{evap}) is given by

$$Q_{conv} = A_{sk} h_c (T_{sk} - T_{amb}) \quad (5)$$

$$Q_{rad} = A_{sk} h_r (T_{sk} - T_{mrt}) \quad (6)$$

$$Q_{evap} = A_{sk} h_e w (P_{sk} - P_{amb}) \quad (7)$$

where A_{sk} is the exposed skin surface area according to Saloum et al. (2007), h_c , h_r , and h_e are the corresponding convective, radiative and evaporative heat transfer coefficients obtained from de Dear et al. (1997), T_{mrt} is the mean radiant temperature, w is the skin wettedness, and P_{sk} and P_{amb} are the water vapor pressures at skin (T_{sk}) and ambient temperature (T_{amb}). Importantly, during the simulations the subjects are assumed to be unclothed. In our simulations, no sweating was considered, so that the skin wettedness was 0.06.

Finally, the arterial and venous blood flow entering the considered segment through the inlet artery/vein vessel ($\dot{m}_{bl,a}$ and $\dot{m}_{bl,v}$), facilitate heat exchanges between the adjacent and considered body segment given as $Q_{adj,a} = \dot{m}_{bl,a} c_{bl}(T_{bl,a,adj} - T_{bl,a})$ and $Q_{adj,v} = \dot{m}_{bl,v} c_{bl}(T_{bl,v,adj} - T_{bl,v})$, where $T_{bl,a,adj}$ and $T_{bl,v,adj}$ are the temperatures of the adjacent artery and vein vessels, respectively. The mean skin temperature ($T_{sk,mean}$) was calculated by summing the products of local skin temperatures and the corresponding weighting factors $k_i = A_{sk,i}/A_{sk,tot}$: $T_{sk,mean} = \sum_{i=1}^n k_i \cdot T_{sk,i}$, where $A_{sk,i}$ is the local skin area of the i -th body segment, $A_{sk,tot}$ is the total body area, $T_{sk,i}$ is local skin temperature of the i -th body segment and n is the number of all body segments ($n = 15$). The mean inner temperature ($T_{cr,mean}$) was defined as the average of the core temperatures of the head, chest and pelvis segments (Coccarelli et al. 2016; Olesen 1984).

2.2 Adaptations of the model to simulate post-cardiac arrest care and TTM

To simulate the thermal responses and physiological processes in patients subjected to post-cardiac intensive care, we complement the model with particularities related to this specific clinical conditions, as described in more detail below.

2.2.1 Metabolic heat production

The metabolic heat generation rate M is the sum of the basal value M_0 and the additional (ΔM) part generated in each segment: $M = M_0 + \Delta M$. The basal metabolic rates M_0 were obtained from Saloum et al. (2007). If the tissue temperature differs from the temperature of thermal neutrality (T_0), the metabolic rate varies with temperature and the additional heat gain ΔM may contain three components (Fiala et al. 2012): changes in the basal metabolism (ΔM_0) and additional metabolism generated by shivering (M_{shiv}) and mechanical work (M_{work}): $\Delta M = \Delta M_0 + M_{shiv} + M_{work}$. The last two terms are present in the core nodes only. It should be noted that during intensive care the patient is immobile, therefore $M_{work} = 0$. Moreover, since the patients subjected to TTM are receiving muscle relaxants to prevent shivering, we set $M_{shiv} = 0$ in all our simulations. Due to changes in the segment's core temperatures, basal metabolism rates decrease, as given by the so called Van't Hoff Q10 relation. Specifically, for every 10 °C reduction in the tissue temperature, there is a corresponding reduction in cell metabolism with a factor of 2 (Fiala et al. 1999; Dennis et al. 2003; Janssen et al. 2005):

$$\Delta M_0 = M_0 [2^{(T-T_0)/10} - 1] \quad (8)$$

where T is the actual local tissue temperature and T_0 the local reference temperature (i.e., in thermoneutral conditions). Considering $\Delta M = \Delta M_0$, the metabolic heat generation rate M can be calculated by the following equation:

$$M = M_0 2^{(T-T_0)/10} \quad (9)$$

2.2.2 Blood circulation and the blood flow rates

The blood flow rates in arteries and veins ($\dot{m}_{bl,a}$ and $\dot{m}_{bl,v}$) are calculated from the perfusion rates $\dot{m}_{per,tot}$ of each segment. For peripheral segments (head, hands and feet), the blood entering rate (arterial blood flow) is equal to the blood perfusion rate and the blood exiting rate (venous blood flow). In the other body segments, the arterial blood flow that enters a segment is the sum of the perfusion flow in the considered segment and the arterial blood flow exciting the segment and entering the adjacent segment. The opposite takes place in the veins. The venous blood flow entering a segment is calculated by subtracting the perfusion flow from the exciting venous blood flow of the considered segment.

Similar to the metabolic heat generation rate, the blood perfusion rates in non-neutral conditions or during exercise vary and can be obtained as: $\dot{m}_{per} = \dot{m}_{per,0} + \Delta \dot{m}_{per}$, where $\Delta \dot{m}_{per}$ is a function of the change in metabolism ΔM and $\dot{m}_{per,0}$ is the basal perfusion blood flow rate in thermal

neutrality taken from Salloum et al. (2007). Instead of dealing with blood perfusion rates \dot{m}_{per} , Fiala et al. (1999) define the blood perfusion change with their energy equivalent $\beta = \rho_{bl} c_{bl} \dot{m}_{per}$. Using $\Delta\beta = \mu \Delta M$ with a proportionally constant $\mu = 0.932$ obtained from Stolwijk, the actual local blood perfusion rate can be obtained as: $\beta = \beta_0 + \Delta\beta$.

Apart from the dependency of the skin perfusion rate on variations of the metabolic heat production rate, the skin perfusion blood flow is also controlled by the mechanisms of vasodilation and vasoconstriction, which increase or decrease the blood flow in the skin layers. To model these processes, we follow the control equations proposed by Salloum et al. (2007).

2.2.3 The effect of general anesthesia

Anesthetics induce a decrease in metabolic heat production by roughly 30% (Matsukawa et al. 1995; Severens et al. 2007), which also affects the blood perfusion rates, as explained above. During general anesthesia, also the thermoregulatory control mechanisms are changed. Anesthetics inhibit thermoregulation in a dose-dependent manner (Sessler 1997). Principally, general anesthesia increases the thresholds for sweating 1 °C and lower the thresholds for vasoconstriction and shivering by approximately 2 °C (Sessler 1997), but during general anesthesia shivering is normally suppressed due to the application of muscle relaxants. So, the overall change in metabolic heat production during general anesthesia that incorporates the temperature-dependent metabolic rate (Eq. 9) is defined as:

$$M_{anest} = 0.7M_0 2^{(T-T_0)/10}. \quad (10)$$

2.2.4 Inflammation and hyperthermia after resuscitation from cardiac arrest

After resuscitation from cardiac arrest, patients frequently experience a complex pathophysiologic state, characterized by inflammatory processes and hyperthermia (Gebhardt et al. 2013; Hickey et al. 2000; Suffoletto et al. 2009; Maier et al. 1994; Yamanaka et al. 2019). The peak increase in temperature was observed from 7 to 18 hours with a median around 12 h (Suffoletto et al. 2009; Takino 1991). Regardless of the underlying cause, hyperthermia results from increases in metabolic rate, which generally varies with the severity of the injury from 20% to up to 100% (Parolari et al. 2003; Clifton et al. 1984; Chioleró et al. 1997). According to (Zeiner et al. 2001; Holzer et al. 2002), we propose an empirical description of the temporal increase in the basal metabolic rate due to inflammatory processes, $M_{0,inflamm}(t)$, as follows:

$$M_{0,inflamm}(t) = M_0 \left[1 + g \left(\frac{t^d}{t^d + t_{inf}^d} \right) \right] \quad (11)$$

where M_0 is the basal metabolic rate in thermal neutrality, g is the relative maximal increase in the metabolic rate, whereas $t_{inf} = 4$ and $d = 3$ define the temporal scale and the steepness of the increase of the metabolic rate, respectively. The overall change in metabolic heat production that incorporates the temporal increase in the metabolic rate due to inflammatory processes (Eq. 11) and the temperature-dependent metabolic rate (Eq. 9), can then be defined as:

$$M_{inflamm}(t) = M_0 2^{(T-T_0)/10} \left[1 + g \left(\frac{t^d}{t^d + t_{inf}^d} \right) \right]. \quad (12)$$

If the patient is additionally exposed to general anesthesia, the overall relative change in metabolic heat production can be calculated by the following equation:

$$M_{sum}(t) = 0.7M_0 2^{(T-T_0)/10} \left[1 + g \left(\frac{t^d}{t^d + t_{inf}^d} \right) \right]. \quad (13)$$

During inflammatory processes, the target core temperature is set to a higher temperature. As a result, the thermoregulatory response thresholds (sweating and vasoconstriction thresholds) are increased. To roughly coincide with the data in Lenhardt et al. (1999), we propose an empirical functional description for the sweating and vasoconstriction thresholds due to different rates of infections and systematic inflammations g , T_{vaso} and T_{sweat} , as follows:

$$T_{vaso} = T_{vaso,init} + (k_{vaso} \frac{g}{g + g_t}) \quad (14)$$

$$T_{sweat} = T_{sweat,init} + (k_{sweat} \frac{g}{g + g_t}) \quad (15)$$

where $T_{vaso,init}$ and $T_{sweat,init}$ are the vasoconstriction/sweating threshold at normal thermoregulation (in case that inflammation occurred in absence of anesthesia) or vasoconstriction/sweating threshold defined during anesthesia (in case of inflammation during anesthesia). In Eq. 14 and Eq. 15, k_{vaso} and k_{sweat} indicate the absolute changes in the threshold temperatures and the g_t reflects the steepness. All these parameters were determined to mimic the data in Lenhardt et al. (1999). Specifically, in case of fever, the values were $T_{vaso,init} = 36.8$ °C, $T_{sweat,init} = 37.1$ °C, $k_{vaso} = 3.5$ °C, $k_{sweat} = 3.5$ °C and $g_t = 0.5$. If inflammation occurred during anesthesia, the values were $T_{vaso,init} = 34.8$ °C, $T_{sweat,init} = 38.1$ °C, $k_{vaso} = 7.0$ °C, $k_{sweat} = 2.5$ °C and $g_t = 0.5$.

2.2.5 The effect of supine body position

In supine position, a large part of the body surface is in direct contact with the bed/mattress. Therefore, the human body can be divided into two parts—one in contact with a bed and the other not. The body part, which is not in contact with a bed, loses heat through skin to the environment by convection, radiation and evaporation:

$$Q_{loss,amb} = (1 - \alpha)(Q_{conv} + Q_{rad} + Q_{evap}) \quad (16)$$

while the heat loss to the environment for the body part in contact with the bed occurs through conduction:

$$Q_{loss,bed} = \alpha Q_{cond} = \alpha \frac{\lambda A(T_{sk,bed} - T_{amb})}{d} \quad (17)$$

where factor $\alpha = 0.39$ defines the body part that is in contact with the bed (Lan et al. 2018). $T_{sk,bed}$ is the skin temperature of the body part that is in contact with the bed. Lan et al. (2018) measured this temperature and showed that the skin temperature was increased by about 0.8 °C compared to those body parts that are not in contact with a bed. The thermal conductivity $\lambda = 0.048$ W/(mK) and thickness $d = 0.2$ m was used in the calculations (Lan et al. 2018). Besides, different heat transfer coefficients have been determined by Kurazumi et al. (2008) and Quintela et al. (2004) for different body positions. For a person in supine position a value of 3.235 W/(m²K) for radiative heat transfer coefficient is suitable (Kurazumi et al. 2008), while the convective heat transfer coefficient can be determined by $h_c = 2.48(T_{sk} - T_{amb})^{0.18}$ (Quintela et al. 2004).

2.2.6 Reduced respiratory heat losses

If the patient breaths with help of a ventilator, the respiratory heat losses are significantly diminished (Marini et al. 1985). In our simulations, we considered this reduction by lowering the respiratory heat loss Q_{res} by 30%.

2.2.7 Targeted temperature management

Surface cooling To simulate the surface body cooling through cooling pads placed on the chest and thighs (30–40% of the total body surface area), we assume a cooling power of $Q_{surface} = 60$ W (Bogerd et al. 2010). The total cooling power is proportionately distributed over the surface area of the chest and thighs segments.

Intravenous infusion of cold saline solution To reduce the patient's temperature via an intravenous route, a rapid infusion of 4 °C cold saline solution is infused through a peripheral intravenous catheter over a definite period. The

heat transfer between the vein blood node in the left upper arm segment and the saline infusion with the coolant flow rate being \dot{V}_{saline} is given by

$$Q_{infusion} = \rho_{saline} c_{saline} \dot{V}_{saline} (T_{saline} - T_{bl,v}) \quad (18)$$

where ρ_{saline} is the saline solution density (rounded to 1000 kg/(m³)), c_{saline} (4200 J/(kgK)) the specific heat of the saline solution and T_{saline} the temperature of the saline solution (Rosengart et al. 2009). We considered an average infusion rate of 80 mL/min.

Esophageal heat transfer device The EHTD is a triple-port, disposable tube made of medical-grade silicone, connected to an external heat exchange unit (Cincinnati Sub-Zero BlanketrolII/III Hyper-Hypothermia System) which circulates cool or warm water through the EHTD via two water ports in closed circuit within the outer lumen of the tube (Hegazy et al. 2015; Markota et al. 2016; Williams et al. 2016). The third central gastric port is isolated and allows suction and decompression of the stomach. The device is placed similarly to a standard orogastric tube, through the mouth into the esophagus to a depth of approximately 45 cm. The device provides cooling via closed-loop system temperature-controlled water circulation, and the temperature of the circulating water is properly adjusted to reach the desired temperature of the patient. The equation that defines the heat transfer rate between the EHTD and the patient (Q_{eso}), where heat is exchanged in a radial direction through the cylindrical configuration, is given by

$$Q_{eso} = 2\pi L_{sil} \frac{T_i - T_o}{\frac{\ln(r_o/r_i)}{\lambda_{sil}} + \frac{\ln(r_i/r_o)}{\lambda_{tissue}}} \quad (19)$$

where L_{sil} is the length of the EHTD placed inside the patient ($L_{sil} = 0.45$ m), T_i is the temperature at the inner surface of the device (the temperature of the circulating water), T_o is the temperature at the outer surface of the device (the temperature of the corresponding segment and node), r_o is the radius of the outer surface (6 mm), and r_i is the radius of the inner surface of the device (5.35 mm), and $\lambda_{sil} = 0.15$ W/(mK) and $\lambda_{tissue} = 0.5$ W/(mK) are the thermal conductivities of the silicone and the surrounding tissue, respectively. By this means, the heat is assumed to be transferred from the circulating water along the device and the surrounding tissue, i.e., the esophagus and the stomach wall, whereby $r_i = r_o + d_{tissue}$ and d_{tissue} is the average thickness of the surrounding tissue (10 mm). Moreover, in our simulations we neglect the heating of the circulating water. By considering the placement of the EHTD from the mouth to the esophagus, the following distribution percentages of the heat transfer rate between the device and the patient can be made: 20% in the head, 50% in the chest and 30% in the pelvis body

segment. The heat exchange is further divided into the core, arterial blood and vein blood node in equivalent parts.

Gastric cooling with ice slurry To simulate the gastric cooling of patients with ice slurry, we propose the use of a balloon catheter (Stull 2006). The balloon catheter is positioned in the stomach of the patient and filled with ice slurry. The heat exchange between the ice slurry and the core of the pelvis segment is given by

$$Q_{iceslurry} = 4\pi\lambda_{tissue} \frac{T_{slurry} - T_{cr,pelvis}}{\frac{1}{r_b} - \frac{1}{r_b + d_{stomach}}} \quad (20)$$

where $\lambda_{tissue} = 0.5 \text{ W/(mK)}$ is the thermal conductivity of the tissue, $T_{cr,pelvis}$ is the core temperature in the pelvis segment, T_{slurry} is the temperature of ice slurry (or water, when the ice melts), r_b is the radius of the inner surface of the balloon catheter (between 5.5 cm and 6.9 cm, depending on the quantity of ice slurry) and d_{tissue} is the thickness of the stomach (10 mm).

3 Results

First, we simulated the evolution of the temperature in different body segments in a patient under general anesthesia. The results are presented in Fig. 2. Initially (in the first hour, i.e., $t < 0$), before any kind of modifications were made, the steady state values at the ambient temperature

of $T_{amb} = 23^\circ\text{C}$ and relative humidity $RH = 45\%$ were obtained. Note that the same protocol was used in all simulations. The onset of anesthesia occurred at $t = 0$, when the thresholds for vasoconstriction and shivering were accordingly reduced for 2°C , the threshold for sweating increased for 1°C and the basal metabolism lowered for 30% (Eq. 10). In the first phase, i.e., 30–45 minutes after anesthesia administration, a redistribution of body heat from the core to the peripheral compartment was observed, resulting in a rapid drop in the average temperature of the inner body of $0.5 - 1^\circ\text{C}$ and a rise in the average skin temperature of around 0.7°C . In this phase, the internal core and skin temperatures of the extremities increased. Afterward, the core as well as the peripheral temperatures decreased due to the negative heat balance and after roughly 2–3 hours the body core temperature stabilized around 35°C . These findings roughly match with previous observations and measurements (Lenhardt 2018; Matsukawa et al. 1995; Bindu et al. 2017).

Next, we simulated the onset of fever as a result of an acute-phase response to infection or systemic inflammation. In these circumstances, the thermoregulatory control system is adjusted to increase body temperature to match a higher set point and an increased heat production is activated (Roth et al. 2006; Moriyama et al. 1999). Both of these features have been incorporated in our model by means of an empirical functional description for the sweating and vasoconstriction thresholds as well as for the evolution of increased

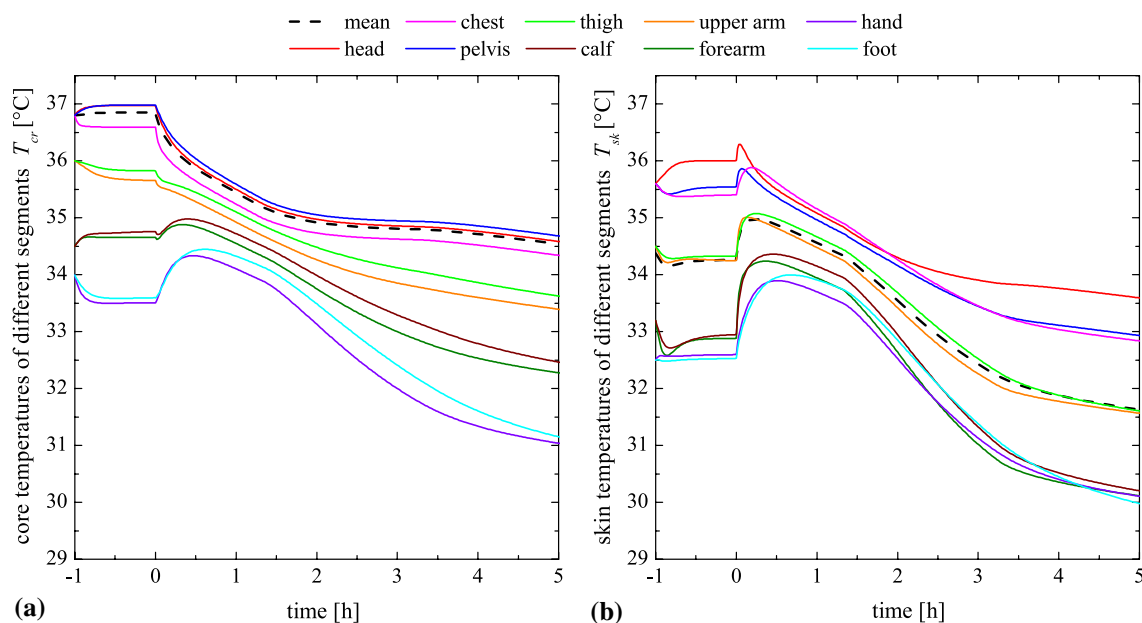


Fig. 2 Predicted evolution of inner core (a) and skin (b) temperatures of different body segments of a nude human body in supine position under general anesthesia. In the first hour (i.e., $t < 0$), the steady-state values at the ambient temperature of $T_{amb} = 23^\circ\text{C}$ and relative

humidity $RH = 45\%$ were obtained. At the time $t = 0$, anesthesia was induced and simulated by reduction of the thresholds for vasoconstriction and shivering for 2°C , by increase of the threshold for sweating for 1°C and a decrease in metabolic heat production by 30%

metabolism. We are of course aware that it is impossible to predict how exactly different levels infections and systematic inflammations affect these thresholds and basal metabolism rates (see Eqs. 12, 14 and Eq. 15), but with this somehow speculative description we tried to fit the model to the available data (Lenhardt et al. 1999). The results in Fig. 3a present the temporal evolution of the body core temperature (pelvis segment) for different changes of the metabolic rate g , i.e., different levels of inflammation. The parameter g signifies the relative change in metabolic heat production, so that, for example, $g = 0.2$ means a 20% increase of the basal metabolism. To provide a better insight, we additionally shown in Fig. 3b the corresponding cross sections for nine different changes of metabolic rate. It can be seen that the increase in the core body temperature monotonically depends on the level of inflammation and that a 20% and 60% increases in metabolism leads to fever and high fever ($> 39^\circ\text{C}$), respectively. In contrast, lower levels of basal metabolism results in lowering of the core temperature, which occurs with a few hours of delay.

In what follows, we examined the evolution of core body temperature during post-resuscitation care in patients after out-of-hospital cardiac arrest (OHCA) who have a return of spontaneous circulation. The modern treatment of cardiac arrest patients encompasses a series of medical procedures with a rapidly changing array of therapeutic approaches. In the last two decades, TTM has become a standard in treating of patients after resuscitation from cardiac arrest. In practice, patients successfully resuscitated from OHCA are subjected to TTM already in the prehospital phase to minimize

reperfusion injury. They may be treated with some cold fluid infusion, while paying attention to fluid overload, and simple external methods, such as cooling blankets or icepacks traditionally placed on groins, armpits and neck (Taccone et al. 2020; Nolan et al. 2015). After admission to hospital, the TTM is continued with supervised cold fluid infusions and surface cooling methods until a series of diagnostic and/or interventional procedures (e.g., usually coronary angiography, echocardiography, and brain and thorax computer tomography) are performed to quickly find and/or treat the underlying pathology. It is also directed at preventing recurrent arrest, thus improving immediate and long-term outcome. During this period, temperature management is hindered. Afterward, the patient is admitted to ICU, where he is further subjected to TTM. Which methods are used to this purpose typically relies on local experience and logistics. It should be noted that during all these processes, patients are receiving anesthetic agents (e.g., dosage adapted to maintain a Richmond Agitation-Sedation Scale score of -4) and muscle relaxants to prevent shivering. Furthermore, we assumed that all patients breath with the help of a ventilator, which significantly diminishes the respiratory heat losses. Due to TTM before the patients are admitted to ICU, and since the systemic inflammatory response has not fully developed, their core body temperature upon arrival to the ICU is usually lower than normal. Cooling namely suppresses many of the pathways associated with ischemia-reperfusion injury, including apoptosis, and the harmful release of excitatory amino acids and free radicals.

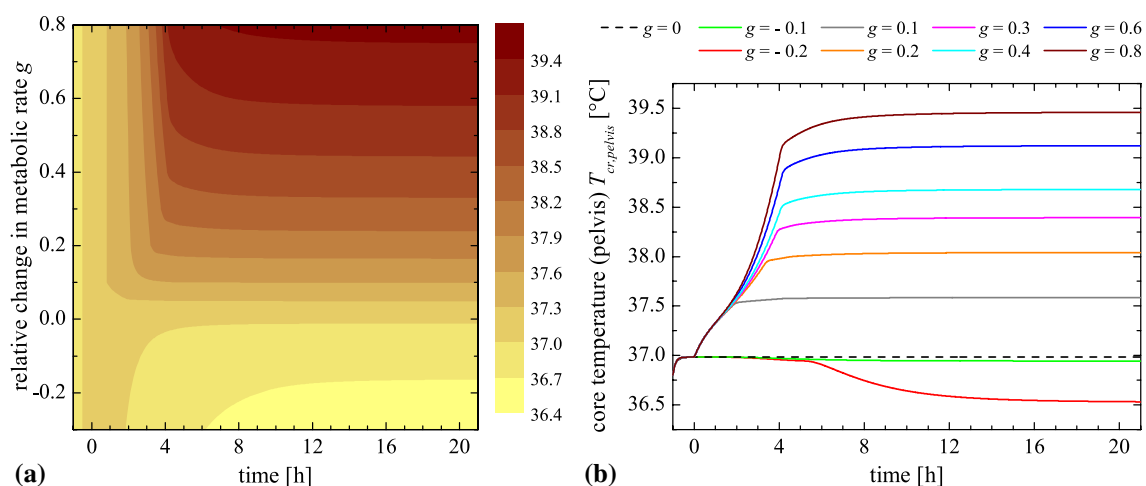


Fig. 3 Depicted is the temporal evolution of body core temperature as a response to changes in the metabolic rate due to inflammatory processes (as specified by Eq. 12). In the left panel (a) the color map encodes the simulated core temperature (pelvis segment) $T_{cr,pelvis}$ as a function of time and the relative maximal change in the metabolic rate g , which is altered from -0.3 to $+0.8$, i.e., -30% to $+80\%$ from the basal value. In the right panel (b) the time course of the simu-

lated $T_{cr,pelvis}$ for nine different values of g is depicted. The dashed black line represents the scenario with an unaltered basal metabolic rate ($g=0$). In the simulations different sweating and vasoconstriction thresholds have been used according to Eq. 14 and Eq. 15. In all cases a nude human body in supine position is assumed, and the ambient temperature $T_{amb} = 23^\circ\text{C}$ and relative humidity $RH = 45\%$ are constant

To incorporate these circumstances in our model, we have used the following protocol in our further simulations. After return of spontaneous circulation ($t = 0$), patients were anesthetized and treated with cold intravenous infusion (300 mL with an infusion rate of 80 mL/min) and surface cooling procedures ($Q_{\text{surface}} = 60$ W) as described in the Mathematical model section, which persisted until the patient was not admitted to a hospital (30 minutes). Right afterward, patients received another dosage of cold fluid infusion (1000 mL with an infusion rate of 80 mL/min) and are additionally cooled with cooling pads. After these further 30 minutes, diagnostic procedures were performed, during which no TTM is possible (60 minutes) and after that patients were transferred to the ICU where TTM via the esophageal cooling device was established, i.e., 2 hours after resuscitation. It can be observed that by this means the model predicts a core temperature prior TTM in the ICU around 35.8 °C, which is consistent with the average temperatures that are in these conditions measured in patients (Holzer et al. 2002; Goury et al. 2017). It should be noted that we implemented a standard protocol for a typical patient, which is consistent with clinical practice guidelines (Callaway et al. 2015) and matches the average behavior observed in reality. However, the timing and the procedures in the prehospital and pre-ICU phases can vary significantly and depend on various

circumstances, which we will address in more detail in continuation.

In Fig. 4a we first show the evolution of the core temperature in the pelvis segment if no further TTM would be performed after 2 hours, when the patient is admitted to the ICU. Simulations are performed for six different increases of metabolic rates due to inflammatory processes (see Eq. 12). The sweating and vasoconstriction thresholds for particular levels of inflammation have been calculated as specified in Eqs. 14 and 15. If there are weak inflammatory processes which enhance the metabolic rate for 10%, the temperature gradually decreases due to anesthetic medications and after around 8 hours the temperature drops below 35 °C. For a 20% increase in metabolic heat production, the core temperature begins slowly to increase. With increasing levels of inflammation, the rising of the temperature becomes progressively more pronounced, leading to hyperthermia. We proceed by investigating the evolution of the body temperature during TTM via the EHTD presented in Fig. 4b. The initial treatment of the patient was the same as described above (the pre-ICU phase) in order to attain 35.8 °C in the core of the pelvis segment before cooling with the EHTD was established. In the simulations, an additional heat flux Q_{eso} was introduced to the head, chest and pelvis body segments, as described in the Mathematical model section. The temperature of the

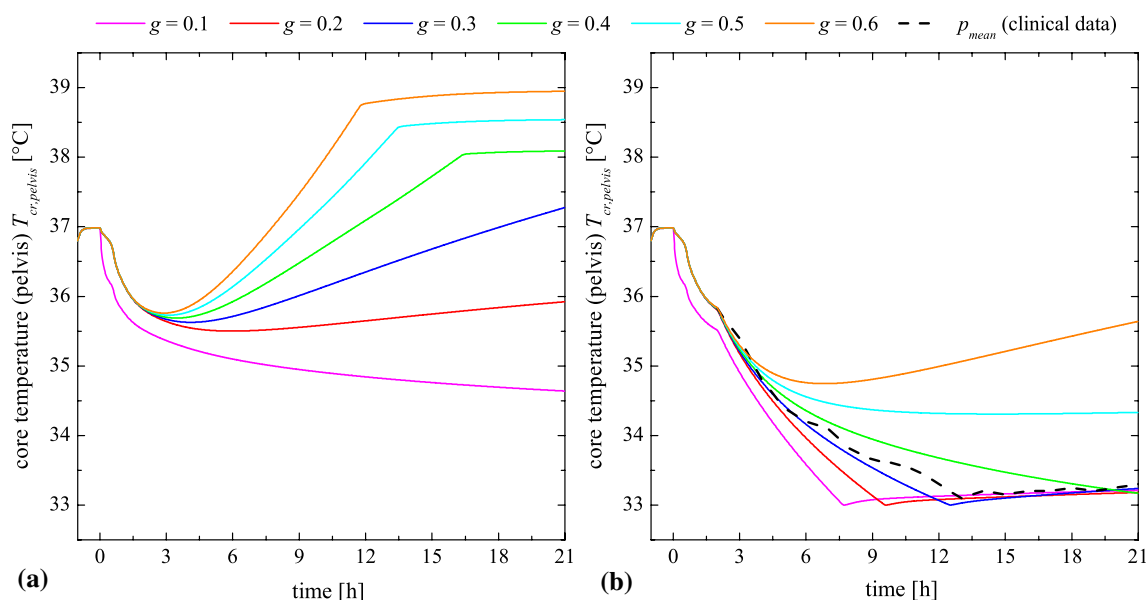


Fig. 4 Presented is the effect of the relative increase in the metabolic rate g due to inflammatory processes during general anesthesia (as specified by Eq. 13) on the core temperature of the pelvis segment after a successful resuscitation after cardiac arrest followed by routine initial assessment and treatment to prevent hyperthermia (see main text for details). Panel (a) shows simulated results for six different relative increases in metabolic rates g , where after admission to the ICU no additional TTM was performed. Panel (b) shows simulated results for the same six different values of g as in panel (a) in com-

parison with measured realistic data from Goury et al. (2017), where after admission to the ICU the patients were additionally cooled via the EHTD. The black dashed line (p_{mean}) represents the evolution of the average temperature of 14 patients included in the study. A nude human body in supine position under general anesthesia, who breaths with help of a ventilator, is assumed in all simulations. The ambient temperature $T_{\text{amb}} = 23$ °C and relative humidity $RH = 45\%$ are constant during the whole simulation

circulating water was $T_i = 4\text{ }^{\circ}\text{C}$ if $T_{cr,pelvis} > 33\text{ }^{\circ}\text{C}$ and was accordingly increased once the desired core temperature was achieved in order to maintain the $T_{cr,pelvis}$ around $33\text{ }^{\circ}\text{C}$, which roughly resembles real circumstances. In Fig. 4b the evolution of the core body temperature $T_{cr,pelvis}$ is shown for six different levels of inflammation. A gradual temperature drop can be observed after the TTM via the esophageal cooling device is initiated. If the level of inflammation is low, i.e., a 10% or 20% increase in the basal metabolic rate, it takes 3–4 hours for the temperature to drop below $34\text{ }^{\circ}\text{C}$ and then additional 3–4 hours to reach the targeted temperature of $33\text{ }^{\circ}\text{C}$. With increasing levels of inflammation, the time in which hypothermia is achieved progressively prolongs and in case of severe inflammation, i.e., a 50% or more increase in the basal metabolic rate, the mild hypothermic state cannot be achieved and in the highly severe case ($g = 0.6$) the body temperature even slowly increases despite TTM. We compare these results with realistic data extracted from Goury et al. (2017). The black dotted line in Fig. 4b shows the evolution of the average temperature of 14 patients. It can be seen that our model prediction matches well the measured data when intermediate levels of inflammation are considered, i.e., a 30–40% increase in the basal metabolic rate. In this case, the average cooling rates were around $0.36\text{ }^{\circ}\text{C/h}$ and $0.25\text{ }^{\circ}\text{C/h}$ to achieve $34\text{ }^{\circ}\text{C}$ and $33\text{ }^{\circ}\text{C}$, respectively.

Next, we investigate how variations in the timing and the procedures in the prehospital and pre-ICU phases affect the evolution of the core body temperature, as in practice a high degree of variability can be noted in this part of the post-cardiac arrest treatment. For this purpose, we simulate the evaluation of the core body temperature in different scenarios. Specifically, we consider two alternative timings: (i) In the fast scenario, the patient had a cardiac arrest relatively close to the hospital and besides basic diagnostics, no additional procedures were required. The timing, in this case, is as follows: 15 minutes between return of spontaneous circulation and hospital administration and additional 30 minutes of diagnostic procedures, which was then immediately followed by TTM via the esophageal cooling device, i.e., 45 minutes after resuscitation. (ii) In the slow scenario, the patient is from a remote place and the transport time to the hospital is 60 minutes. After administration, the patient was subjected to 150 minutes of intensive diagnostic procedures and interventions, so that TTM via the esophageal cooling device in the ICU occurred 210 minutes after resuscitation. Furthermore, we additionally examine the influence of cold fluid infusion. In the first case, no cooling with cold intravenous infusion is applied, for example, due to the patient's previous history of heart disease (i.e., heart failure) and the possible additional risks, this might provide (i.e., lung edema). In the second case, a maximal dosage of cold saline was considered (2000 mL instead of 1000 mL in the

standard protocol). The results with the standard value of increased metabolic heat production ($g = 0.3$) are presented in Fig. 5. It can be observed that between these scenarios there can be up to a 4-hour difference in the time required to achieve hypothermia. The effect of cold saline infusions in the pre-hospital setting has been previously explored (Rajek et al. 2000). Numerically it appears to have an important role as a variable. Nevertheless, the adverse effects of the rapid infusion of cold intravenous fluids in the prehospital setting must be weighed against the potential positive effect (Callaway et al. 2015).

Finally, we additionally explore an alternative method to reduce the body temperature during the post-cardiac arrest care. Specifically, we simulate the thermal behavior of a patient subjected to gastric cooling with ice slurry via a special tube (see the Mathematical model section for further details). Noteworthy, gastric cooling offers some advantages in comparison with standard procedures. First, a gastric balloon catheter is relatively easy to insert and is in comparison to other semi-invasive methods more practical, as there are no power sources and controls required and can thus be utilized already during the first hour of treatment, when the patient requires diagnostic and therapeutic procedures. Second, due to a larger available surface area for heat transfer, absorption of latent heat and the proximity to the core

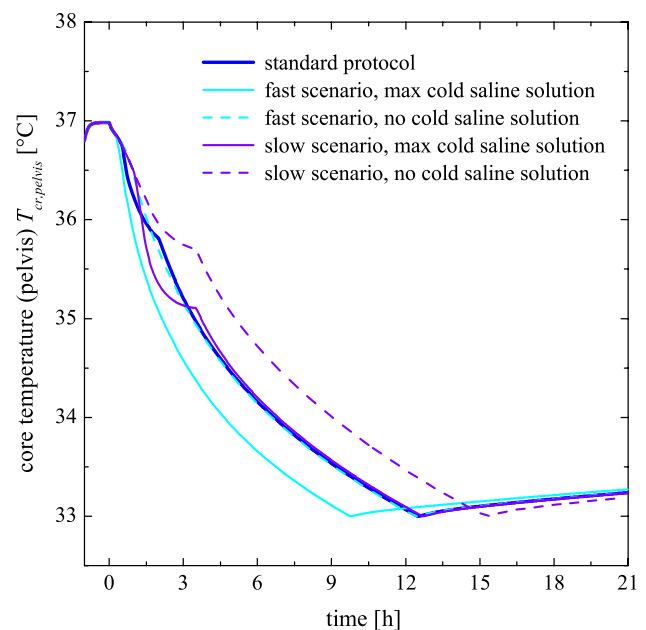


Fig. 5 Shown is the temporal evolution of the core temperature of the pelvis segment after return of spontaneous circulation in different pre-ICU scenarios and cold saline infusion protocols (see main text for further details). In all cases an intermediate increase in metabolic rate due to inflammatory processes was considered ($g = 0.3$) and all other parameter values and protocols were the same as in Fig. 4. The full blue line represents the results obtained with the standard protocol (the same as in Fig. 4b)

organs, a faster effect might be expected. The later would be particularly desirable, because with more conventional methods, such as the EHTD, the cooling is fairly slow. To investigate this issue, we first performed simulations with different masses of ice slurry in a patient with an intermediate level of inflammation ($g = 0.4$). Gastric cooling was initiated 30 minutes after the admission to the hospital, 1 hour after resuscitation. Otherwise, the protocol before the ICU phase was the same as described above, except that gastric cooling was initiated earlier in the process when compared to TTM via the EHTD, i.e., already during diagnostic and therapeutic procedures. The results in Fig. 6a reveal that the body core temperature drops quite rapidly and proportional to the quantity of ice slurry. The decrease in temperature is particularly fast in the first 30 min, before the ice melts. In case of a probably most realistic scenario with 0.75 kg of ice slurry, the average cooling rate in the first two hours was around 0.8°C/h . However, the absolute decrease of the core temperature in this case is only around 1.5°C . If the quantity of ice slurry is increased to 1.0 kg, the body core temperature decreased only for an additional 0.5°C . We next investigated how the evolution of the core temperature in the pelvis segment depends on the level of inflammation. In the simulation, we have used 0.75 kg of ice slurry and the results are presented in Fig. 6b. It appears that the severity of inflammation only weakly affects this initial drop of temperature. This is a rather expected results, as in these relatively early stages after a successful resuscitation, the

inflammatory activity has not yet completely evolved (see Fig. 3). Finally, we examine the effect of two successive inductions of ice slurry ($m_{\text{slurry}} = 0.75\text{ kg}$) in a patient that evolves an intermediate inflammatory response ($g = 0.4$). The results in Fig. 6c indicate that in this case the body core temperature can fall below 33.5°C in 2 hours, i.e., with a very high average cooling rate of 1.5°C/h . However, after around 4 hours after the second induction of ice slurry, the temperature again rises above 34°C , which implies that other TTM strategies should be used after that to keep the patient in hypothermic state.

4 Discussion

Temperature management is a frequently used therapeutic modality in medicine. Especially in a clinical setting, the precise regulation of body temperature in the form of TTM is an instrumental part of hospital intensive care (Cariou et al. 2017; Andrews et al. 2018; Skok et al. 2020). Inducing mild regulated hypothermia to counteract severe hyperthermia that develops after return of spontaneous circulation due to the post-cardiac arrest syndrome has been a part of therapeutic guidelines for almost two decades. This management has been associated with better neurological outcomes and reduced mortality rates (Bernard et al. 2002; Callaway et al. 2015; Holzer et al. 2002). However, the thermodynamic homeostasis in such patients is very complex and

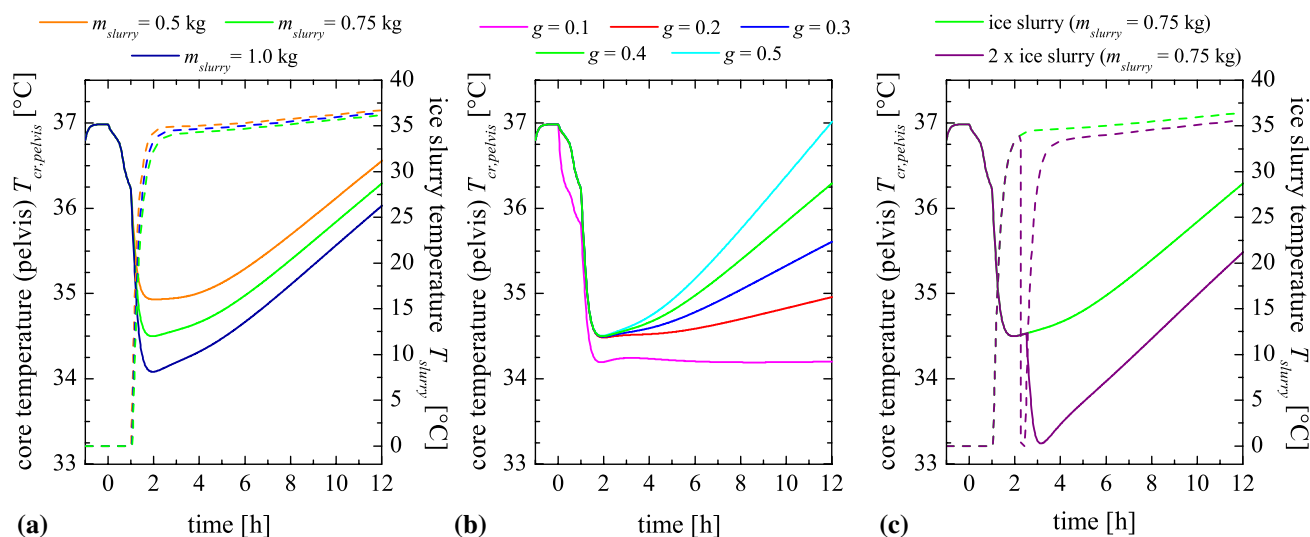


Fig. 6 Depicted is the temporal evolution of body core temperature of the patient's body core temperature (pelvis segment), where after the pre-ICU phase (for details see the Results section) gastric cooling with ice slurry was performed. In panel (a) the time course of the simulated core temperature of the pelvis segment $T_{cr,pelvis}$ (left axis) and the ice slurry temperature T_{slurry} (right axis) for three different masses of ice slurry m_{slurry} and an intermediate level of inflammation ($g = 0.4$) are presented. Panel (b) shows simulated results for a

fixed amount of ice slurry ($m_{slurry} = 0.75\text{ kg}$) for five different levels of inflammation g . In panel (c) simulated results for one (green lines) and two (purple lines) successive inductions of 0.75 kg ice slurry, in patients with an intermediate level of inflammation ($g = 0.4$), are depicted. In all cases a nude human body in supine position under general anesthesia, who breaths with help of a ventilator, is assumed, and the ambient temperature $T_{amb} = 23^\circ\text{C}$ and relative humidity $RH = 45\%$ are constant

affected by numerous factors. It is therefore difficult to predict the patient's responses and the underlying evolution of the body temperature with regard to different circumstances and strategies, which can be employed for TTM. In the present study, we aimed to investigate these issues and improve our understanding of the relationship between the patient's thermal behavior and treatment strategies, by designing a computational bioheat model that incorporates the crucial elements related to these specific clinical circumstances. In this regard, we have utilized a well-established biothermal model of the human body and upgraded it by incorporating: (1) a temperature-dependent basal metabolism and blood flow-rates, (2) the effect of anesthesia and muscle relaxants, (3) inflammatory processes occurring after resuscitation, (4) body position (e.g., supine), (5) respiratory support, and (6) different TTM strategies.

In our simulations, we first calculated the evolution of the patient's body temperature under anesthesia. The results predicted a three-phasic response, i.e., a redistribution of body heat from the core to the peripheral compartment within the first hour, an overall decrease of body temperature for the next two hours, and a final temperature stabilization around 34.5 °C, which is well in agreement with previous observations and measurements (Lenhardt 2018; Matsukawa et al. 1995; Bindu et al. 2017). Then, we simulated the onset of fever as a result of the post-cardiac arrest syndrome as well as a response to infection. We modeled this by means of an empirical functional description for the sweating and vasoconstriction thresholds as well as for the evolution of increased heat production. How exactly the thermoregulatory control system operates in these circumstances is incompletely understood, but we attempted to fit our model to the limited available data (Lenhardt et al. 1999), which yielded reliable results. Next, we focused on the evolution of the body temperature in a patient subjected to post-resuscitation care. To this purpose, we included in our simulations a typical protocol that encompassed anesthesia and TTM with cold intravenous infusion and surface cooling procedures, partly in the prehospital phase, which was then followed by TTM in the ICU. Particular emphasis was given to temperature regulation via an EHTD. Our results for this approach and when modeling intermediate levels of inflammation were in accordance to already published experimental observation data (Goury et al. 2017). Furthermore, in patients with a weak inflammatory response, mild hypothermia was achieved faster, whereas for severe systemic inflammation, the desired temperatures below 35 °C could not be achieved. This can potentially serve as an indication for the utilization of additional cooling strategies in such circumstances. Moreover, the evolution of the core body temperature was found to be affected by the timing and the procedures in the prehospital and pre-ICU phases as well, which can vary significantly due to practical reasons (i.e.,

logistics). Our results suggest that when the transportation and the treatment of a patient after return of spontaneous circulation require more time, the utilization of additional cooling techniques in the pre-ICU phase, such as cold intravenous infusions numerically lead to a faster temperature maintenance initiation. Nevertheless, we want to stress that additional rapid infusion of intravenous fluids was not associated with improved survival or neurologic recovery. The decision for an additional fluid infusion must be made with care and on a case-by-case basis (Callaway et al. 2015; Bernard et al. 2016). Finally, we theoretically examined an alternative approach to induce mild hypothermia. This method is called ice slurry gastric cooling and is not part of clinical practice. Potential benefits of this method include its relative simplicity compared with other semi- and invasive methods, as insertion of a gastric tube is a routine low risk procedure, additional external control after connecting it to an external regulator would be minimized and in principle the procedure could be employed much earlier, (i.e., already in the out-of-hospital setting). The net benefit is an extended cooling time frame which includes the prehospital, preadmission phase and diagnostic/therapeutic phase at admission. Notably, our computational results showed that a gastric balloon catheter filled with ice slurry is a very efficient method to rapidly lower the core temperature. By utilizing this method, hypothermia can be induced much faster when compared to cooling via the EHTD (same circumstances).

Post-resuscitation care is a rapidly developing field. Changes of a number of treatment strategies have over the past two decades led to gradually improved survival rates of OHCA patients, although the overall survival rates remain rather low (Myat et al. 2018). Improvements during the past two decades include, in addition to TTM, a higher rate of bystander CPR, higher rate of bystander use of automatic external defibrillators, a more aggressive approach to hemodynamic stabilization and support, and a more thorough initial diagnostic workup, all of which affect survival (Sasson et al. 2010; Wissenberg et al. 2013). While the current international guidelines advocate for TTM, it is not entirely clear to what extent therapeutic mild hypothermia outperforms the maintaining of normothermia (Nielsen et al. 2013). In contrast, in different animal models the positive effect of hypothermia on the outcome is much more evident (Abella et al. 2004; Wang et al. 2010). It might be argued that these indistinct differences between mild hypothermia and fever prevention only strategy in humans stem from too slow cooling rates, which can typically be achieved in clinical practice. Moreover, even though the individual phases of patient care rely on speed and accuracy, it is fact that during certain timeframes (e.g., prehospital, diagnostic and/or interventional procedures at admission) adequate TTM simply is not fully possible. In some previous studies, the administration of cold intravenous fluids was found to be an efficient way

to swiftly reduce the core temperatures (Bernard and Rosalio 2008; Arulkumaran et al. 2012; Markota et al. 2015, 2016), but due to possible adverse effects associated with fluid overload it is advised against it, particularly in the less supervised and probably more crucial pre-admission phases (Callaway et al. 2015). Therefore, gastric cooling with ice slurry might be a viable alternative, as it has proven efficacy in animal (Hoek et al. 2004) and human (Siegel et al. 2010) testing, due to a stronger cooling capacity per unit volume. This implies faster cooling rates, which would be particularly desirable, as conventional methods, such as the EHTD, induce hypothermia rather slowly. This was also predicted by our numerical simulations.

Even though the core multimode computational model we used is based on well-established bioheat transfer analyses (Salloum et al. 2007), including well-specified physiological parameters and thermal properties, our study has inherent limitations. Our aim was to principally simulate the behavior in an average patient undergoing standard post-resuscitation care. However, the later can significantly vary between patients, as the timing and treatment strategies depend on external circumstances, such as the ambulance response time and geographical location (Lyon et al. 2004), differences in emergency medicine service systems organization, staffing and logistics (DeLia et al. 2015), etc. These factors affect the course of thermal activity within a patient. Furthermore, the interpatient variability is striking. Factors such as gender, age, body mass index, body segment proportions, pharmacological interventions are known to affect the physiological thermoregulatory mechanisms, vasomotor functions and heat transfer within the body (Havenith 2001; Zhang et al. 2001; Rida et al. 2014; Hristov 2019). The patient's thermal state in the ICU also depends on the environmental conditions, the severity of underlying pathology, other medical conditions, etc. (Moriyama et al. 1999; Severens et al. 2007; Niven and Laupland 2016; Romadhon et al. 2017). While it is clear that infection and sickness lead to an increase in temperature and the resting metabolic rate (Demas et al. 1997; Otálora-Ardila et al. 2016), the degree depends on the severity and exhibits interpatient variability (Maier et al. 1994; Gassen et al. 2022). Notably, various aspects of these complex issues have also been studied by computational models (McDaniel et al. 2019; Yamanaka et al. 2019; Orłowski et al. 2014; Dobрева et al. 2021). Moreover, simulating the heat flow between the cooling device and the human body is a very complex undertaking, and it is impossible to provide a comprehensive description of all the processes that take place in reality. Esophageal and gastric mucosa may have unexpected behavior when exposed to cold and locally temperature gradients and blood flow rates might be reduced, which limits the amount of heat that can be extracted in vivo (Vaicys et al. 2012). Moreover, the physical contact between the cooling device and the surrounding tissue is not perfect

and depends also on the anatomy of the patient. All these factors affect heat transfer efficacy. Finally, for some specific aspects of our model, there is only limited data available, which allowed us only an empirical description of relations between certain parameters, as already outlined above.

Nevertheless, our goal was not to provide an ultimate description of the patient's thermoregulation in the ICU. Rather, we aimed to provide a theoretical basis that incorporates many genuine features which affect the human heat balance during TTM after successful resuscitation from cardiac arrest. Utilizing this framework, we could not only rather firmly simulate the patient's thermal behavior TTM after resuscitation, but also determine to what extent different levels of inflammation contribute to the variable responses to thermal treatment and theoretically evaluate a possible new cooling method, i.e., gastric cooling with ice slurry. Future efforts should aim to incorporate individual patient characteristics and consider measuring multiple physiological parameters to better calibrate computational bioheat models. The recently emerging fields of network physiology and network medicine could provide the necessary means to better assess the interorgan relationships and predict the responses to TTM and other critical care interventions (Ivanov et al. 2016; Asada et al. 2016; Moorman et al. 2016). Perhaps the interplay between computational modeling and advances in smart bio-measurement technologies will play a key role in optimizing TTM strategies in a variety of clinical circumstances, even though there is still a rather long way to go before such approaches will become widespread in clinical practice.

Acknowledgements The authors acknowledge the financial support from the Slovenian Research Agency (Grant Nos. J1-2457, J1-9112, P1-0403, P3-0396 and J3-3077).

Declarations

Conflict of interest The authors declare no competing interests.

References

- ASHRAE (2001) Handbook of Fundamentals (American Society of Heating, Atlanta, Refrigerating and Air Conditioning Engineers, p 2001
- Abella BS, Zhao D, Alvarado J, Hamann K, Hoek TLV, Becker LB (2004) Intra-arrest cooling improves outcomes in a murine cardiac arrest model. *Circulation* 109:2786
- Alves EC, Mady CEK (2020) Thermodynamic assessment of therapeutic hypothermia techniques for rehabilitation of post-cardiac arrest patients. *Case Stud Therm Eng* 22:100752
- Andrews PJD, Verma V, Healy M, Lavinio A, Curtis C, Reddy U, Andrzejowski J, Foulkes A, Canestrini S (2018) Targeted temperature management in patients with intracerebral haemorrhage, subarachnoid haemorrhage, or acute ischaemic stroke: consensus recommendations. *Br J Anaesth* 121:768

- Arulkumaran N, Suleman R, Ball J (2012) Use of ice-cold crystalloid for inducing mild therapeutic hypothermia following out-of-hospital cardiac arrest. *Resuscitation* 83:151
- Asada T, Aoki Y, Sugiyama T, Yamamoto M, Ishii T, Kitsuta Y, Nakajima S, Yahagi N, Doi K (2016) Organ system network disruption in nonsurvivors of critically ill patients. *Crit Care Med* 44:83
- Avolio AP (1980) Multi-branched model of the human arterial system. *Med Biol Eng Comput* 18:709
- Badjatia N, Gupta N, Sanchez S, Haymore J, Tripathi H, Shah R, Hannan C, Tandri H (2020) Safety and feasibility of a novel transnasal cooling device to induce normothermia in febrile cerebrovascular patients. *Neurocrit Care*. <https://doi.org/10.1007/s12028-020-01044-9>
- Bernard SA, Gray TW, Buist MD, Jones BM, Silvester W, Gutteridge G, Smith K (2002) Treatment of comatose survivors of out-of-hospital cardiac arrest with induced hypothermia. *N Engl J Med* 346:557
- Bernard SA, Rosalion A (2008) Therapeutic hypothermia induced during cardiopulmonary resuscitation using large-volume, ice-cold intravenous fluid. *Resuscitation* 76:311
- Bernard SA, Rosalion K, Finn J, Hein C, Grantham H, Bray JE, Deasy C, Stephenson M, Williams TA, Straney LD et al (2016) Induction of therapeutic hypothermia during out-of-hospital cardiac arrest using a rapid infusion of cold saline: the RINSE trial (rapid infusion of cold normal saline). *Circulation* 134:797
- Bindu B, Bindra A, Rath G (2017) Temperature management under general anesthesia: compulsion or option. *J Anaesthesiol Clin Pharmacol* 33:306
- Bogerd N, Psikuta A, Daanen HA, Rossi RM (2010) How to measure thermal effects of personal cooling-systems: human, thermal manikin and human simulator study. *Physiol Meas* 31:1161
- Bräuer A, Pacholik L, Perl T, English MJM, Weyland W, Braun U (2004) Conductive heat exchange with a gel-coated circulating water mattress. *Anesth Analg* 99:1742
- Callaway CW, Donnino MW, Fink EL, Geocadin RG, Golan E, Kern KB, Leary M, Meurer WJ, Peberdy MA, Thompson TM et al (2015) Part 8: Post-cardiac arrest care: 2015 American heart association guidelines update for cardiopulmonary resuscitation and emergency cardiovascular care. *Circulation* 132:S465
- Cariou A, Payen JF, Asehnoune K, Audibert G, Botte A, Brissaud O, Debaty G, Deltour S, Deye N, Engrand N et al (2017) (2017), Targeted temperature management in the ICU: guidelines from a French expert panel. *Ann Intensive Care* 7:1–14
- Chioléro R, Revelly J-P, Tappy L (1997) Energy metabolism in sepsis and injury. *Nutrition* 13:45
- Clifton GL, Robertson CS, Grossman RG, Hodge S, Foltz R, Garza C (1984) The metabolic response to severe head injury. *J Neurosurg* 60:687
- Coccarelli A, Boileau E, Parthimos D, Nithiarasu P (2016) An advanced computational bioheat transfer model for a human body with an embedded systemic circulation. *Biomech Model Mechanobiol* 15:1173
- DeLia D, Wang HE, Wang J, Merlin M, Nova J, Lloyd K, Cantor JC (2015) Prehospital transportation to therapeutic hypothermia centers and survival from out-of-hospital cardiac arrest Pre-hospital transportation to therapeutic hypothermia centers and survival from out-of-hospital cardiac arrest. *BMC Health Serv Res* 15:1–9
- de Dear RJ, Arens E, Hui Z, Oguro M (1997) Convective and radiative heat transfer coefficients for individual human body segments. *Int J Biometeorol* 40:141
- Demas GE, Chefer V, Talan MI (1997) Nelson RJ (1997), Metabolic costs of mounting an antigen-stimulated immune response in adult and aged C57BL/6J mice, *American Journal of Physiology-Regulatory, Integrative and Comparative Physiology* 273
- Dennis BH, Eberhart RC, Dulikravich GS, Radons SW (2003) Finite-element simulation of cooling of realistic 3-D human head and neck. *J Biomech Eng* 125:832
- Dobrev A, Brady-Nicholls R, Larripa K, Puelz C, Mehlsen J, Olufsen MS (2021) A physiological model of the inflammatory-thermal-pain-cardiovascular interactions during an endotoxin challenge. *J Physiol* 599:1459
- Donnino MW, Andersen LW, Berg KM, Reynolds JC, Nolan JP, Morley PT, Lang E, Cocchi MN, Xanthos T, Callaway CW et al (2015) Temperature management after cardiac arrest: an advisory statement by the advanced life support task force of the international liaison committee on resuscitation and the American heart association emergency cardiovascular care committee and the council on cardiopulmonary. *Crit Care Perioper Resusc Circ* 132:2448
- Enescu D (2019) Models and indicators to assess thermal sensation under steady-state and transient conditions. *Energies* 12:841
- Faridi P, Prakash P (2018) In experimental validation of computational models of microwave tissue heating with magnetic resonance thermometry. In: 2018 IEEE/MTT-S international microwave symposium - IMS
- Fiala D, Havenith G, Bröde P, Kampmann B, Jendritzky G (2012) UTCI-Fiala multi-node model of human heat transfer and temperature regulation. *Int J Biometeorol* 56:429
- Fiala D, Lomas KJ, Stohrer M (1999) A computer model of human thermoregulation for a wide range of environmental conditions: the passive system. *J Appl Physiol* 87:1957
- Fiala D, Psikuta A, Jendritzky G, Paulke S, Nelson DA, Lichtenbelt WDM, Frijns AJH (2010) Physiological modeling for technical, clinical and research applications. *Front Biosci Sch* 2(S3):939
- Fu M, Weng W, Chen W, Luo N (2016) Review on modeling heat transfer and thermoregulatory responses in human body. *J Therm Biol* 62:189
- Fuentes D, Oden JT, Diller KR, Hazle JD, Elliott A, Shetty A, Stafford RJ (2009) Computational modeling and real-time control of patient-specific laser treatment of cancer. *Ann Biomed Eng* 37:763
- Gagge AP, Stolwijk J, Nishi Y (1971) An effective temperature scale based on a simple model of human physiological regulatory response. *ASHRAE Trans* 77:247
- Gassen J, Nowak TJ, Henderson AD, Muehlenbein MP (2022) Dynamics of temperature change during experimental respiratory virus challenge: Relationships with symptoms, stress hormones, and inflammation. *Brain Behav Immun* 99:157
- Gebhardt K, Guyette FX, Doshi AA, Callaway CW, Rittenberger JC, Service PCA (2013) Prevalence and effect of fever on outcome following resuscitation from cardiac arrest. *Resuscitation* 84:1062
- Goury A, Poirson F, Chaput U, Voicu S, Garçon P, Beeken T, Malissin I, Kerdjane L, Chelly J, Vodovar D et al (2017) Cooling methods of targeted temperature management and neurological recovery after out-of-hospital cardiac arrest: a nationwide multicenter multi-level analysis. *Resuscitation* 121:54
- Havenith G (2001) Individualized model of human thermoregulation for the simulation of heat stress response. *Journal of applied physiology* 90:1943
- Hegazy A, Lapierre D, Althenayan E (2015) Targeted temperature management after cardiac arrest and fever control with an esophageal cooling device. *Crit Care* 19:424
- Hegazy AF, Lapierre DM, Butler R, Martin J, Althenayan E (2017) The esophageal cooling device: a new temperature control tool in the intensivist's arsenal. *Heart Lung* 46, 143
- Hensley DW, Mark AE, Abella JR, Netscher GM, Wissler EH, Diller KR (2013) 50 years of computer simulation of the human thermoregulatory system. *J Biomech Eng* 135:021006

- Hickey RW, Kochanek PM, Ferimer H, Graham SH, Safar P (2000) Hypothermia and hyperthermia in children after resuscitation from cardiac arrest. *Pediatrics* 106:118
- Hoek TLV, Kasza KE, Beiser DG, Abella BS, Franklin JE, Oras JJ, Alvarado JP, Anderson T, Son H, Wardrip CL et al (2004) Induced hypothermia by central venous infusion: saline ice slurry versus chilled saline. *Crit Care Med* 32:S425
- Holopainen R (2012) Ph.D. thesis, A human thermal model for improved thermal comfort, Technical Research Centre of Finland
- Holzer M, Sterz F, Darby JM, Padosch SA, Kern KB, Böttiger BW, Polderman KH, Girbes ARJ, Holzer M, Bernard SA et al (2002) Mild therapeutic hypothermia to improve the neurologic outcome after cardiac arrest. *N Engl J Med* 346:549
- Hristov J (2019) Bio-heat models revisited: Concepts, derivations, nondimensionalization and fractionalization approaches, *Frontiers in Physics* 7
- Ivanov PC, Liu K (2016) Bartsch RP (2016) Focus on the emerging new fields of network physiology and network medicine. *New journal of physics* 18
- Janssen FE, Leeuwen GMV, Steenhoven AAV (2005) Modelling of temperature and perfusion during scalp cooling. *Phys Med Biol* 50:4065
- Jiang YY, Yanai E, Nishimura K, Zhang H, Abe N, Shinohara M, Wakatsuki K (2010) An integrated numerical simulator for thermal performance assessments of firefighters' protective clothing. *Fire Saf J* 45:314
- Kaddi CD, Phan JH, Wang MD (2013) Computational nanomedicine: modeling of nanoparticle-mediated hyperthermal cancer therapy. *Nanomedicine* 8:1323
- Katič K, Li R, Zeiler W (2016) Thermophysiological models and their applications: a review. *Build Environ* 106:286
- Khan I, Haymore J, Barnaba B, Armahizer M, Melnosky C, Bautista MA, Blaber B, Chang WT, Parikh G, Motta M et al (2018) Esophageal cooling device versus other temperature modulation devices for therapeutic Normothermia in subarachnoid and intracranial hemorrhage. *Ther Hypothermia Temp Manag* 8:53
- Kim KH, Shin SD, Song KJ, Ro YS, Kim YJ, Hong KJ, Jeong J, Park JH, Kim TH, Kong SY (2018) Cooling methods of targeted temperature management and neurological recovery after out-of-hospital cardiac arrest: a nationwide multicenter multi-level analysis. *Resuscitation* 125:56
- Koelblen B, Psikutaa A, Bogdan A, Annaheim S, Rossi RM (2017) Thermal sensation models: a systematic comparison. *Indoor Air* 27:680
- Kurazumi Y, Tsuchikawa T, Matsubara N, Horikoshi T (2008) Effect of posture on the heat transfer areas of the human body. *Build Environ* 43:1555
- Lan L, Zhai ZJ, Lian Z (2018) A two-part model for evaluation of thermal neutrality for sleeping people. *Build Environ* 132:319
- Lascarrou J-B, Merdji H, Gouge AL, Colin G, Grillet G, Girardie P, Coupez E, Dequin P-F, Cariou A, Boulain T et al (2019) Targeted temperature management for cardiac arrest with nonshockable rhythm. *N Engl J Med* 381:2327
- Lenhardt R, Negishi C, Sessler DI, Ozaki M, Ettinger K, Bastanmehr H, Lobo E (1999) The effect of pyrogen administration on sweating and vasoconstriction thresholds during desflurane anesthesia. *Anesthesiology* 90:1587
- Lenhardt R (2018) In Chapter 37 - body temperature regulation and anesthesia, thermoregulation: from basic neuroscience to clinical neurology, Part II. In: Romanovsky AA (eds) *Handbook of clinical neurology*. Elsevier, Amsterdam, pp 635–644
- Leong SH, Chan E, Ho BC, Yeo C, Lew S, Sewa DW, Lim SL, Lee CW, Chia PL, Lim TS et al (2017) Therapeutic temperature management (TTM): post-resuscitation care for adult cardiac arrest, with recommendations from the National TTM Workgroup. *Singapore Med J* 58:408
- Lyon RM, Cobbe SM, Bradley JM, Grubb NR (2004) Surviving out of hospital cardiac arrest at home: a postcode lottery? *Emerg Med J* 21:619
- Maier SF, Watkins LR, Fleshner M (1994) Psychoneuroimmunology The interface between behavior, brain, and immunity. *Am Psychol* 49:1004
- Marini JJ, Capps JS, Culver BH (1985) The inspiratory work of breathing during assisted mechanical ventilation. *Chest* 87:612
- Markota A, Fluher J, Kit B, Balažič P, Sinkovič A (2016) The introduction of an esophageal heat transfer device into a therapeutic hypothermia protocol: a prospective evaluation. *Am J Emerg Med* 34:741
- Markota A, Gosak M, Duh M, Skok K (2022) Temperature management and its role in cardiac arrest patients a review. *Signa Vitae* 1:8
- Markota A, Palfy M, Stožer A, Sinkovič A (2015) Difference between bladder and esophageal temperatures in mild induced hypothermia. *J Emerg Med*. <https://doi.org/10.1016/j.jemermed.2014.12.059>
- Matsukawa T, Sessler DI, Sessler AM, Schroeder M, Ozaki M, Kurz A, Cheng C (1995) Heat flow and distribution during induction of general anesthesia. *Anesthesiology* 82:662
- McDaniel M, Keller JM, White S (2019) A. Baird, A Whole-Body Mathematical Model of Sepsis Progression and Treatment Designed in the BioGears Physiology Engine, *Frontiers in Physiology* 10 (2019)
- Moorman JR, Lake DE, Ivanov P (2016) Early detection of sepsis-A role for network physiology? *Crit Care Med* 44:e312
- Moriyama S, Okamoto K, Tabira Y, Kikuta K, Kukita I, Hamaguchi M, Kitamura N (1999) Evaluation of oxygen consumption and resting energy expenditure in critically ill patients with systemic inflammatory response syndrome. *Crit Care Med* 27:2133
- Morrison SF, Nakamura K (2019) Central mechanisms for thermoregulation. *Annu Rev Physiol* 81(1):285
- Myat A, Song K-J, Rea T (2018) Out-of-hospital cardiac arrest: current concepts. *Lancet* 391:970
- Naiman MI, Gray M, Haymore J, Hegazy AF, Markota A, Badjatia N, Kulstad EB (2017) Esophageal heat transfer for patient temperature control and targeted temperature management. *J Vis Exp: JOVE* 129:56579
- Naiman M, Shanley P, Garrett F, Kulstad E (2016) Evaluation of advanced cooling therapy's esophageal cooling device for core temperature control. *Expert Rev Med Devices* 13:423
- Neimark MA, Konstant AA, Choi JH, Laine AF, Pile-Spellman J (2008) Brain cooling maintenance with cooling cap following induction with intracarotid cold saline infusion: a quantitative model. *J Theor Biol* 253:333
- Nguyen PL, Alreshaid L, Poblete RA, Konye G, Marehbian J, Sung G (2018) Targeted temperature management and multimodal monitoring of comatose patients after cardiac arrest. *Front Neurol* 9:768
- Nielsen N, Wetterslev J, Cronberg T, Erlinge D, Gasche Y, Hassager C, Horn J, Hovdenes J, Kjaergaard J, Kuiper M et al (2013) Targeted temperature management at 33 °C versus 36 °C after cardiac arrest. *N Engl J Med* 369:2197
- Niven DJ (2016) Laupland KB (2016) Pyrexia: aetiology in the ICU. *Critical Care* 20
- Nolan JP, Soar J, Cariou A, Cronberg T, Moulart VR, Deakin CD, Bottiger BW, Friberg H, Sunde K, Sandroni C (2015) European resuscitation council and European society of intensive care medicine 2015 guidelines for post-resuscitation care. *Intensive Care Med* 41:2039
- Nolan JP, Soar J, Cariou A, Cronberg T, Moulart VR, Deakin CD, Bottiger BW, Friberg H, Sunde K, Sandroni C (2015) European resuscitation council and European society of intensive care medicine guidelines for post-resuscitation care 2015: section 5

- of the European resuscitation council guidelines for resuscitation 2015. *Resuscitation* 95:202
- Olesen BW (1984), *How Many Sites Are Necessary to Estimate a Mean Skin Temperature* (New York, Raven Press, 1984)
- Orlowski P, McConnell FK, Payne S (2014) A mathematical model of cellular metabolism during ischemic stroke and hypothermia A mathematical model of cellular metabolism during ischemic stroke and hypothermia. *IEEE Trans Biomed Eng* 61:484
- Orthaber K, Pristovnik M, Skok K, Perić B, Maver U (2017) Skin cancer and its treatment: novel treatment approaches with emphasis on nanotechnology. *J Nanomater* 2017:2606271
- Otálora-Ardila A (2016) M LGH, Flores-Martínez JJ, Metabolic KCW Jr (2016) Cost of the Activation of Immune Response in the Fish-Eating Myotis (*Myotis vivesi*): The Effects of Inflammation and the Acute Phase Response. *PLoS ONE* 11:1
- Parolari A, Alamanni F, Juliano G, Polvani G, Roberto M, Veglia F, Fumero A, Carlucci C, Rona P, Brambillasca C et al (2003) Oxygen metabolism during and after cardiac surgery: role of CPB. *Ann Thorac Surg* 76:737
- Pennes HH (1948) Analysis of tissue and arterial blood temperature in the resting human forearm. *J Appl Physiol* 1:93
- Prakash P, Salgaonkar VA, Diederich CJ (2013) Modelling of endoluminal and interstitial ultrasound hyperthermia and thermal ablation: applications for device design, feedback control and treatment planning. *Int J Hypertherm* 29:296
- Quintela D, Gaspar A, Borges C (2004) Analysis of sensible heat exchanges from a thermal manikin. *Eur J Appl Physiol* 92:663
- Rajek A, Greif R, Sessler DI, Baumgardner J, Laciny S, Bastanmehr H (2000) Core cooling by central venous infusion of ice-cold (4°C and 20°C) fluid: isolation of core and peripheral thermal compartments. *Anesthesiology* 93:629
- Raouf I, Khalid S, Khan A, Lee J, Kim HS, Kim MH (2020) A review on numerical modeling for magnetic nanoparticle hyperthermia: progress and challenges. *J Therm Biol* 91:102644
- Rida M, Ghaddar N, Ghali K, Hoballah J (2014) Elderly bioheat modeling: changes in physiology, thermoregulation, and blood flow circulation. *Int J Biometeorol* 58:1825
- Romadhon R, Rinata AD, Suprijanto Bindar Y, Soelami FXN (2017) Development of thermoregulation model of surgical patient and heat exchange with air condition in the operating room. *Procedia Eng* 170:547
- Rosengart AJ, Zhu L, Schappeler T, Goldenberg FD (2009) Simple intravenous fluid regimens to control fever in hospitalized stroke patients: a theoretical evaluation. *J Clin Neurosci* 16:51
- Roth J, Rummel C, Barth SW, Gerstberger R, Hübschle T (2006) Molecular aspects of fever and hyperthermia. *Neurol Clin* 24:421
- Salloum M, Ghaddar N, Ghali K (2007) A new transient bioheat model of the human body and its integration to clothing models. *Int J Therm Sci* 46:371
- Sasson C, Rogers MA, Dahl J, Kellermann AL (2010) Predictors of survival from out-of-hospital cardiac arrest: a systematic review and meta-analysis. *Circ Cardiovasc Qual Outcomes* 3:63
- Sessler DI (1997) Mild perioperative hypothermia. *N Engl J Med* 336:1730
- Severens NMW, Lichtenbelt WDvM, Frijns AJH, Steenhoven AAV, de Mol BAJM, Sessler DI, (2007) A model to predict patient temperature during cardiac surgery. *Phys Med Biol* 52:5131
- Shafirstein G, Feng Y (2013) The role of mathematical modelling in thermal medicine. *Int J Hyperthermia* 29:259
- Shrivastava D (2018) Theory and applications of heat transfer in humans. Wiley, Burnsville
- Siegel R, Maté J, Brearley MB, Watson G, Nosaka K, Laursen PB (2010) Ice slurry ingestion increases core temperature capacity and running time in the heat. *Med Sci Sports Exerc* 42:717
- Silva ABCG, Wrobel LC, Ribeiro FLB (2018) A thermoregulation model for whole body cooling hypothermia. *J Therm Biol* 78:122
- Skok K, Duh M, Markota A, Gosak M (2020) Thermoregulation: a journey from physiology to computational models and the intensive care unit. *Wiley Interdiscip Rev Syst Biol Med* 13(4):e1513
- Stolwijk JAJ (1970) In physiological and behavioral temperature regulation In: Hardy JD, Gagge AP and Stolwijk JAJ (eds) Charles C. Thomas Publishing Company, pp 703–721
- Stull PM (2006) Method for gastric cooling using balloon catheter. U.S. Patent 7,077,825 B1, Jan 2006
- Suffoletto B, Peberdy MA, van der Hoek T, Callaway C (2009) Body temperature changes are associated with outcomes following in-hospital cardiac arrest and return of spontaneous circulation. *Resuscitation* 80:1365
- Suriyanto NEYK, Kumar SD (2017) Physical mechanism and modeling of heat generation and transfer in magnetic fluid hyperthermia through Néelian and Brownian relaxation: a review. *Biomed Eng Online* 16:36
- Taccone FS, Picetti E, Vincent JL (2020) High quality targeted temperature management (TTM) after cardiac arrest. *Critical Care* 24:1–7
- Takino MOY (1991) Hyperthermia following cardiopulmonary resuscitation. *Intensive Care Med* 17:419
- Tansey EA, Johnson CD (2015) Recent advances in thermoregulation. *Adv Physiol Educ* 39(3):139
- Tindall MJ, Peletier MA, Severens NMW, Veldman DJ, de Mol BAJM (2008) Understanding post-operative temperature drop in cardiac surgery: a mathematical model. *Math Med Biol* 25:323
- Vaicys V, Eason A, Schieber JD, Kulstad EB (2012) Therapeutic hypothermia induction via an esophageal route - a computer simulation. *Am J Emerg Med* 30:932
- Vallez LJ, Plourde BD, Abraham JP (2016) A new computational thermal model of the whole human body: applications to patient warming blankets. *Numer Heat Transf A: Appl* 69:227
- Vanlandingham SC, Kurz MC, Wang HE (2015) Thermodynamic aspects of therapeutic hypothermia. *Resuscitation* 86:67
- Wakamatsu H, Utsuki T (2009) Development of a basic air-cooling fuzzy control system for hypothermia. *Artif Life Robot* 14:311
- Wang H, Barbut D, Tsai MS, Sun S, Weil MH, Tang W (2010) Intra-arrest selective brain cooling improves success of resuscitation in a porcine model of prolonged cardiac arrest. *Resuscitation* 81:617
- Wang N, Liu Q, Shi Y, Wang S, Zhang X, Han C, Wang Y, Cai M, Ji X (2021) Modeling and simulation of an invasive mild hypothermic blood cooling system. *Chin J Mech Eng* 34:1–9
- Wang L, Yin H, Di Y, Liu Y, Liu J (2016) Human local and total heat losses in different temperature. *Physiol Behav* 157:270
- Weng WG, Han XF, Fu M (2014) An extended multi-segmented human bioheat model for high temperature environments. *Int J Heat Mass Transf* 75:504
- Williams D, Leslie G, Kyriazis D, O Donovan B, Bowes J, Dingley J (2016) Use of an esophageal heat exchanger to maintain core temperature during burn excisions and to attenuate pyrexia on the burns intensive care unit. *Case Reports in Anesthesiology* 2016:7306341
- van Willigen BG, Otterspoor LC, van Veer M, Rosalina TT, Pijls NHJ, van de Vosse FN (2019) A predictive computational model to estimate myocardial temperature during intracoronary hypothermia in acute myocardial infarction. *Med Eng Phys* 68:65
- Wissenberg M, Lippert FK, Folke F, Weeke P, Hansen CM, Christensen EF, Jans H, Hansen PA, Lang-Jensen T, Olesen JB et al (2013) Association of national initiatives to improve cardiac arrest management with rates of bystander intervention and patient survival after out-of-hospital cardiac arrest. *JAMA* 310:1377
- Xue X, Liu J (2011) Multi-scale modeling on human intravascular cooling to induce brain hypothermia via circle of Willis. *Forsch Ingenieurwes* 75:257

- Yamanaka Y, Uchida K, Akashi M, Watanabe Y, Yaguchi A, Shimamoto S, Shimoda S, Yamada H, Yamashita M, Kimura H (2019) Mathematical modeling of septic shock based on clinical data. *Theor Biol Med Model* 16:1–22
- Zeiner A, Holzer M, Sterz F, Schörkhuber W, Eisenburger P, Havel C, Kliegel A, Laggner AN (2001) Hyperthermia after cardiac arrest is associated with an unfavorable neurologic outcome. *Arch Intern Med* 161:2007
- Zhang H, Huizenga C, Arens E, Yu T (2001) Considering individual physiological differences in a human thermal model. *J Therm Biol* 26:401